



# Agglomeration, support effects, and CO adsorption on Au/TiO<sub>2</sub>(1 1 0) prepared by ion beam deposition

Sungsik Lee, Chaoyang Fan, Tianpin Wu, Scott L. Anderson \*

*Department of Chemistry, University of Utah, 315 S. 1400 E. RM Dock, Salt Lake City, UT 84112-0850, United States*

Received 8 October 2004; accepted for publication 6 January 2005

Available online 22 January 2005

## Abstract

The agglomeration behavior of 0.05 ML of Au deposited as Au<sup>+</sup> at 1 eV impact energy on rutile TiO<sub>2</sub>(1 1 0) was investigated by a combination of ion scattering, X-ray photoelectron spectroscopy (XPS), CO adsorption, and CO temperature-programmed desorption (TPD). Samples were studied over the temperature range between 115 K and 800 K, and on both near-stoichiometric UHV-annealed TiO<sub>2</sub>, and TiO<sub>2</sub> with a high density of oxygen vacancies created by He<sup>+</sup> bombardment. At low temperatures, Au is atomically dispersed, shifting into complexes with oxygen vacancies for  $T_{\text{anneal}}$  around room temperature, and finally agglomerating into small clusters for  $T_{\text{anneal}} \geq 450$  K. CO adsorbed on dispersed atoms results in nearly 1 eV shift in the Au 4f binding energy to higher energy, and CO desorption peaking at 280 K. CO adsorbs more weakly on Au–vacancy complexes and on Au in clusters, as indicated by both TPD and XPS. Comparisons with experiments depositing thermal Au, and implications for size-selected CO oxidation on Au<sub>n</sub>/TiO<sub>2</sub> are discussed.

© 2005 Elsevier B.V. All rights reserved.

**Keywords:** Sintering; Ion deposition; CO adsorption

## 1. Introduction

The Au/TiO<sub>2</sub> system has received a great deal of experimental [1–5] and theoretical [6–9] attention in the past few years, because it has been found

to have unique catalytic properties that are strongly dependent on the size/morphology of the supported Au. In addition to size effects, activity of gold catalysts is sensitive to sample preparation and pretreatment conditions [10–14]. Most information regarding size effects on catalytic activity comes from TEM or STM characterization, on catalysts or model catalysts with average particle sizes in the nanometer range [1–3]. These measurements suggest that catalytic activity for a

\* Corresponding author. Tel.: +1 801 585 7289; fax: +1 801 581 8433.

E-mail address: [anderson@chemistry.utah.edu](mailto:anderson@chemistry.utah.edu) (S.L. Anderson).

variety of reactions peaks for particles of a few nanometers diameter, and the particle size trends suggest that activity for molecular scale particles should be low. In contrast, Heiz and co-workers showed that for CO oxidation on  $\text{Au}_n/\text{MgO}$  prepared by size-selected cluster deposition, activity is significant for clusters containing as few as eight atoms [15].

More recently, we studied room temperature CO oxidation on  $\text{Au}_n/\text{TiO}_2$  prepared by size-selected deposition on single crystal rutile  $\text{TiO}_2(110)$  [5]. Weak activity was found for clean  $\text{TiO}_2$ , attributed to reaction at oxygen vacancy defects present on the surface at the 7–10% level. Samples prepared by  $\text{Au}^+$  and  $\text{Au}_2^+$  deposition are far less reactive than clean  $\text{TiO}_2$ , whereas samples prepared by deposition of  $\text{Au}_n^+$ ,  $n \geq 3$  showed substantial activity, with strong dependence on deposited cluster size. These experiments provide indirect insight into the behavior of the gold clusters during and after room temperature deposition, but also raise some interesting questions. The strong and sharp dependence on cluster size was interpreted as indicating that under our deposition conditions, deposited  $\text{Au}_n^+$  do not fragment or agglomerate extensively. The near-zero CO oxidation activity for samples prepared by  $\text{Au}^+$  deposition was proposed to result from Au atoms binding at oxygen vacancies, thereby blocking reactions at the vacancies. This interpretation is consistent with the fact that the  $\text{Au}^+$  deposition density in those studies was sufficient to block all vacancy sites.

The conclusion that gold deposited as  $\text{Au}_n^+$  does not agglomerate at room temperature is inconsistent with STM observations by Mitchell et al. [16] and Wahlstrom et al. [4]. In these experiments, Au was evaporated onto rutile  $\text{TiO}_2(110)$  and surfaces were imaged at different temperatures. Mitchell et al. report 2–3 nm diameter clusters at room temperature, even for coverages well below 0.1 ML. Wahlstrom et al. observed atoms adsorbed at oxygen vacancies and clusters of a few atoms on terrace sites at 130 K. At 300 K, however, clusters with  $\sim 30$  atoms were observed, preferentially adsorbed at step edges.

It is not surprising that evaporated gold atoms should diffuse and agglomerate more readily than

the deposited clusters in our experiment, because the pre-formed clusters have stabilizing Au–Au bonds that would tend to inhibit diffusion. On the other hand, it is not obvious why deposited  $\text{Au}^+$  should have different agglomeration behavior than evaporatively deposited Au. The purpose of this paper is to probe the behavior of deposited  $\text{Au}^+$  over a wide temperature range, using a combination of X-ray photoelectron spectroscopy (XPS), ion scattering spectroscopy (ISS), and CO adsorption. The results are consistent with agglomeration being a minor process for deposited  $\text{Au}^+$  at temperatures of 300 K and below, rapidly becoming important at higher temperatures.

CO adsorption is one of the best studied surface processes, and is a key step in several important reactions (e.g., methanation or CO oxidation). One interesting issue is the electronic interaction of Au and  $\text{Au}_n$  with vacancies, and the effects of this interaction on CO adsorption. The size selected cluster study by Sanchez et al. [15] indicated that charge transfer between clusters and defects on their MgO surface played an important role on the reaction. Arrii et al. [17] also examined the influence of different supports with different levels of vacancies on CO adsorption and oxidation, by deposition of preformed, non-mass-selected clusters, and concluded that vacancies are important. Freund and co-workers [18,19] recently studied CO adsorption behavior on different size gold clusters grown on reducible  $\text{FeO}(111)$ ,  $\text{Fe}_3\text{O}_4(111)$  supports, and on non-reducible  $\text{Al}_2\text{O}_3$ . They concluded that CO adsorption strongly depends on the size of gold clusters, but that the reducibility of the support does not affect the bond strength between the gold particles and the CO molecules. A density functional study of CO oxidation on supported gold particles by Lopez and Nørskov [20] suggests that the reaction center is more related to cluster structure rather than the metal-support interaction. In a similar vein, Gottfried et al. [21] compared CO adsorption behavior on both single crystal gold and on a sputtered gold surface, concluding that the CO adsorption behavior is sensitive to surface structure and coordination number of the surface gold atoms.

## 2. Experimental

The experiments were carried out in a vacuum system consisting of a previously described mass-selected ion deposition beamline [22], coupled to a new ultrahigh vacuum (UHV) end chamber with base pressure  $<2 \times 10^{-10}$  Torr. The UHV chamber incorporates facilities for sample preparation, X-ray photoelectron spectroscopy (XPS), Auger electron spectroscopy (AES), and ion scattering spectroscopy (ISS). It also includes a differentially pumped mass spectrometer (UTI 100C) for temperature programmed desorption/reaction (TPD/TPR) studies. The sample can be inserted through a seal and isolated in a second chamber that serves as a high pressure cell and load-lock. While the end chamber system is new, our operating and analysis procedures are essentially identical to those previously described [23,24].

The TiO<sub>2</sub>(110) single crystal (Commercial Crystal Laboratories) was mounted on a molybdenum back plate (0.2 mm thick) and could be heated up to 1200 K by resistive heating and cooled down to 110 K by direct contact with a liquid nitrogen reservoir. Sample temperatures were measured by a K-type thermocouple attached to the edge of the TiO<sub>2</sub> crystal with UHV compatible ceramic glue (Aremco, Ceramabond 571). The crystal was cleaned by repeated cycles of Ar<sup>+</sup> bombardment and 1100 K annealing, not only removing contaminants, but leaving the crystal with sufficient bulk conductivity to perform electron spectroscopy and ion beam deposition without surface charging problems. The cleanliness of the sample was checked by XPS and ISS before and during deposition experiments. Before gold deposition, the TiO<sub>2</sub> sample was cleaned by bombarding with 1 keV Ar<sup>+</sup> followed by a 15 min annealing period at 850 K in UHV. The state of the surface was probed by Ti XPS and water TPD, both methods indicating that the TiO<sub>2</sub> is nearly stoichiometric with 7–10% surface oxygen vacancies [25]. For comparison, some deposition studies were also performed on a TiO<sub>x</sub> surface where a high level of defects, including oxygen vacancies, was generated by 1 keV He<sup>+</sup> bombardment (600 nA 10 min).

Mass-selected Au<sup>+</sup> was deposited at a deposition energy of 1 eV/atom, on TiO<sub>2</sub> held at 115 K. The Au was deposited in a 2 mm diameter spot, to a density equivalent to 0.05 of a close-packed Au monolayer ( $7.0 \times 10^{13}$  Au/cm<sup>2</sup>), as determined by ion current measurement. Deposition times were 5–10 min. The XPS experiments were carried out using an MgK $\alpha$  (1253.6 eV) X-ray source, and binding energies were calibrated using the O 1s peak of TiO<sub>2</sub>, in turn calibrated against the Au spectrum of gold foil. The spectra shown in the figures have been corrected by subtraction of a Shirley background. Spectral fitting and peak integration was done using the XPSPEAK package [26]. For ISS, He<sup>+</sup> at 1 keV kinetic energy was directed at the sample spot at a 45° angle of incidence, and scattered He<sup>+</sup> was collected along the surface normal, and energy analyzed using the hemispherical analyzer. For CO adsorption studies, <sup>13</sup>C<sup>18</sup>O (ISOTECH) was used without purification. For TPD measurements, the sample was placed in front of the differentially pumped mass spectrometer and heated at a rate of 3 K/s.

## 3. Results and discussion

### 3.1. Ion scattering spectroscopy (ISS) analysis

Fig. 1 shows the results of a series of annealing experiments on a sample prepared by deposition of 5% ML-equivalent of Au<sup>+</sup> on vacuum-annealed TiO<sub>2</sub> at 115 K. After deposition, the samples were annealed for 5 min to the indicated temperatures, re-cooled, then probed by 1 keV He<sup>+</sup> ion scattering. The results are given as the ISS signal for scattering from Au, divided by the sum of the ISS signals for scattering from Ti and O (the “Au/substrate ratio”). This ratio obviously depends on the amount of Au present in the top-most layer of the sample, but the gold over layer also attenuates ISS signal from Ti and O. For our ISS geometry (45° incident angle, collection along the sample normal), attenuation is significant only for Ti and O atoms immediately surrounding the Au adatoms. Attenuation is expected both from scattering by the Au cores (i.e. “shadowing” and “blocking”

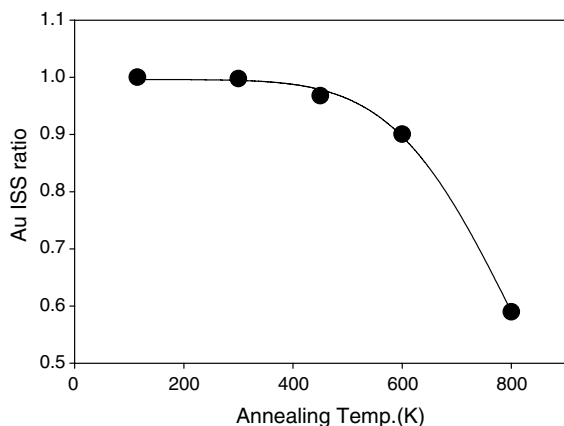


Fig. 1. Dependence of Au/substrate ISS ratio on annealing temperature.

[27]), and from decreased ion survival probability (ISP) in trajectories scattering from substrate atoms such that  $\text{He}^+$  must pass through the Au electron cloud. Because ISP varies for scattering from different types of atoms, it is not possible to interpret the absolute ISS intensities, however, the Au/substrate ratio is sensitive to the gold morphology.

The maximum Au/substrate ratio is expected for atoms dispersed on top of the substrate. Some diminution of the ratio is expected as Au aggregates into 2-d islands, because, although all Au is still in the top layer, the attenuation footprint of neighboring Au atoms will tend to overlap to some extent. For reference, our ISS measurements [28] for small size-selected  $\text{Au}_n^+$  deposited on  $\text{TiO}_2$  show a  $\sim 10\%$  decrease in Au/substrate ratio between  $\text{Au}_1^+$  and  $\text{Au}_2^+$ , with much less change for  $\text{Au}_3^+$  or  $\text{Au}_4^+$ . Large changes in the ratio can occur only if the fraction of the top layer comprised of gold is reduced, i.e., if Au forms multi-layer surface structures, desorbs, or goes subsurface. Examples of these effects can be seen in ISS studies of size-selected  $\text{Ni}_n$  and  $\text{Ir}_n$  clusters on  $\text{TiO}_2$  [23,24].

STM experiments [4] indicate that Au is immobile on  $\text{TiO}_2$  at cryogenic temperatures, thus we interpret the Au/substrate ratio for the as-deposited sample at 115 K as representing dispersed atoms on the surface. As Fig. 1 shows, there is no change in the Au/substrate ISS ratio for anneal-

ing up to room temperature, indicating that most Au is still in the form of isolated atoms. Agglomeration, even into small single-layer clusters, appears to be minimal at room temperature and below. This conclusion is consistent with the results of our CO oxidation study [5], where we found that samples prepared by  $\text{Au}_1$  and  $\text{Au}_2$  deposition at room temperature were inactive, while deposition of  $\text{Au}_3$  or larger clusters resulted in active catalysts. If significant agglomeration of deposited Au atoms occurred at room temperature, it is hard to imagine such sharply size-dependent activity.

The Au/substrate ISS ratio decreases slightly for  $T_{\text{anneal}} = 450$  K, consistent with the onset of agglomeration to single-layer clusters. Again, the ISS observations are consistent with our CO oxidation study, where we found that significant activity could be induced by annealing the catalysts to  $T_{\text{anneal}} \geq 400$  K, presumably because small clusters begin to form. After 600 K annealing, the Au/substrate ratio is still  $\sim 90\%$  of the low  $T_{\text{anneal}}$  value, indicating that most Au is still in the top-most layer, i.e., the gold islands are mostly single layer. After 800 K annealing, the Au/substrate ISS ratio decreases substantially ( $\sim 40\%$ ), indicating that a significant fraction of the gold is no longer in the top-most layer. Thermal desorption of Au can be excluded because there is no decrease in Au XPS intensity following annealing at 800 K. One possible scenario is formation of 3-d particles, with average thickness around two layers. Alternatively, it is possible that high annealing temperature leads to Au particles that are partially covered by  $\text{TiO}_x$ . In any case, for  $T_{\text{anneal}} \leq 600$  K, sintering to 2-d gold particles is sufficient to account for the ISS results.

The idea that cluster size increases with annealing temperature is consistent with STM experiments by Lai et al. [29] and Mitchell et al. [16]. Their results indicate significant growth of Au nanoparticles at  $T \geq 750$  K compared to the particles deposited at room temperature, however, annealing to 650 K did not result in significant changes in the size distribution [29]. STM and computational results of Wahlstrom et al. [4] suggest that 2-d clusters are more stable than 3-d clusters for gold adsorbed on oxygen vacancies.

### 3.2. X-ray photoelectron spectroscopy (XPS) analysis

Fig. 2 shows the results of an analogous series of annealing experiments using XPS to probe changes in the Au chemical environment. The XPS of the as-deposited sample at 115 K is shown as the bottom spectrum. The sample was then annealed at 200 K for 5 min, re-cooled to 115 K, then re-examined by XPS, resulting in the spectrum labeled “200 K”. Spectra taking following analogous five minute annealing experiments at 300 K, 450 K and 600 K, are also shown. Each spectrum

is split into  $4f_{7/2}$  and  $4f_{5/2}$  fine structure components. Spectral fitting was done for both components, however, for simplicity’s sake, binding energy values will be quoted only for the more intense  $4f_{7/2}$  component.

The sample as prepared at 115 K has an average Au $4f_{7/2}$  binding energy of 85.8 eV but the peak is considerably broader (FWHM: 2.4 eV) than our instrumental resolution (1.2 eV) Since Au is immobile at low temperatures, the width of the XPS peak presumably reflects the various geometries where isolated Au atoms are bound. The only change observed after annealing to 200 K is a

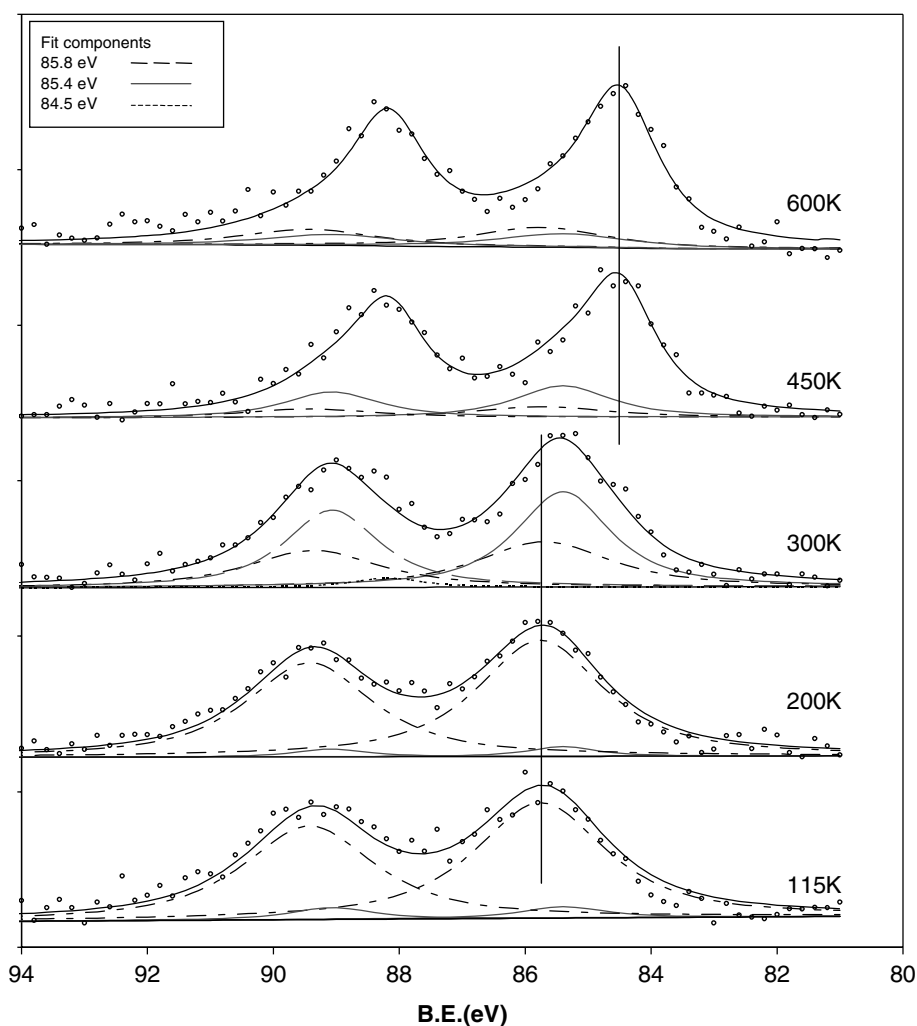


Fig. 2. Au $4f$  XPS for samples annealed to the indicated temperatures. Spectral fitting is described in the text.

slight peak narrowing, suggesting that some of the original binding site dispersion has been annealed away. After annealing to 450 K or 600 K, the peak has narrowed significantly, and shifted to a binding energy of  $\sim 84.5$  eV, with little change between the 450 K and 600 K spectra. Both previous STM experiments [4,16,30] and our ISS results indicate that Au agglomerates into small clusters in this temperature range, thus this 84.5 eV binding energy is assigned to Au in clusters on the TiO<sub>2</sub> surface.

The most interesting spectrum is that taken after annealing to 300 K, i.e., the temperature where we observed strong dependence of catalytic activity on deposited cluster size. The peak position is at 85.4 eV—intermediate between the low temperature and high temperature peak positions. In addition, the peak is asymmetric, with a suggestion of a weak shoulder at  $\sim 84.5$  eV—the high temperature binding energy position attributed to Au in supported clusters.

To extract more quantitative insight, the spectra were fit to linear combinations of individual components. Each component was assumed to be a  $4f_{7/2}$ – $4f_{5/2}$  doublet, with Gaussian–Lorentzian line shapes, relative intensity, and fine structure splitting determined from fitting a spectrum of clean gold foil. The adjustable parameters for each component were taken as the intensity, binding energy, and full width at half maximum (FWHM). The goal of the fitting process was to minimize the number of fit components required. For that reason, the FWHM values for the fit components were allowed to vary, rather than being fixed at the instrumental resolution (1.2 eV). Increased feature width is not unreasonable, particularly for low annealing temperatures, because significant binding site inhomogeneity is expected if mobility is low. For example, even on perfect TiO<sub>2</sub> terraces, density functional calculations have indicated the existence of several stable Au binding sites [6,8,31], and binding at vacancies or step edges is also possible.

We first fit the relatively sharp 450 K and 600 K spectra to a single component with best fit  $4f_{7/2}$  binding energy of 84.5 eV, and FWHM (1.4 eV) only slightly wider than the instrumental limit. The 84.5 eV fit component, therefore, is identified

with gold in environments produced by high temperature annealing, i.e., gold in nanoscale clusters on the surface. This single component fit, based on the instrumental lineshape measured for bulk gold, reproduces the peaks well, but does not adequately fit the intensity tails observed to high binding energy of each fine structure peak. Assignment of a 84.5 eV binding energy to Au in supported gold clusters is consistent with the work of Egdell and co-workers [16,32] who found Au 4f binding energies of  $\sim 84.5$  eV for small Au clusters on TiO<sub>2</sub>.

We next fit the 115 K and 200 K spectra to a single broad component with best fit  $4f_{7/2}$  binding energy of 85.8 eV, and width of 2.4 eV. Because previous STM studies have shown little Au mobility at low temperatures [4], we identify this 85.8 eV component with Au mostly atomically dispersed on the TiO<sub>2</sub> surface, in a distribution of binding sites. The fact that the 200 K spectrum is nearly identical to that at 115 K, indicates that any changes in binding site distribution that occur over this temperature range do not cause significant changes in the XPS chemical shift.

We then tried to fit the 300 K spectrum to a linear combination of the 85.8 eV and 84.5 eV components, however, an adequate two-component fit was not possible. Rather than allowing the component binding energies to shift, we allowed the fitting program to introduce third fit component, with best-fit binding energy of 85.4 eV. This component dominates the XPS fits at 300 K, and because 300 K is where the size-dependent catalytic activity was measured, the interpretation of this 85.4 eV component is important. Additional experiments probing this issue are described below, but we note that both our CO oxidation experiments and the ISS results above, suggest that agglomeration is not a major process at room temperature, i.e., the Au is still mostly isolated. Furthermore, the CO oxidation experiments showed that Au<sup>+</sup> deposited at room temperature poisons CO oxidation that would otherwise occur at oxygen vacancy sites on the TiO<sub>2</sub>. Therefore, we tentatively identify this 85.4 eV feature with Au atoms complexed to oxygen vacancies.

Fig. 2 shows the experimental spectra and the final fits, where each spectrum was fit to a linear combination of the three 85.8, 85.4, and 84.5 eV

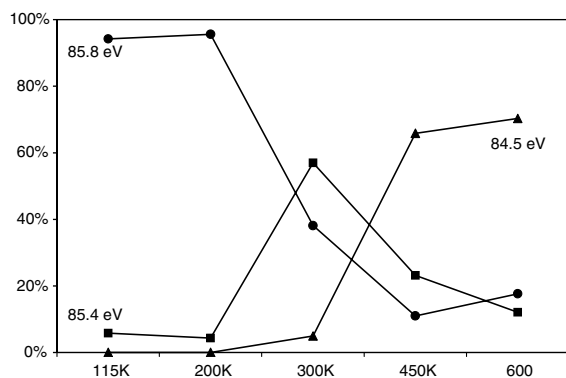


Fig. 3. Contributions from the three fit components for different annealing temperature. (●) 85.8 eV; (■) 85.4 eV; (▲) 84.5 eV.

components, and Fig. 3 gives the contribution of each fit component as a function of temperature. At low temperatures, the Au is almost entirely in the 85.8 eV (atomically-dispersed) state, with ~5–8% contribution from the 85.4 eV component. Given that our surface has vacancy density of 7–10%, this is just about what would be expected if deposited Au<sup>+</sup> binds close to its landing point. At 450 K and above, the gold is mostly present as clusters (84.5 eV), and there is a substantial contribution from the 85.4 eV (vacancy-complex) component only for  $T_{\text{anneal}}$  around 300 K.

XPS binding energies are affected by a combination of so-called initial and final state effects. Initial state effects refer to the fact that the electron binding energy is affected by the local electron density (i.e., net charge) on the atom from which the photoelectron is ejected. For a given core level energy, the photoelectron binding energy is higher for atoms with net positive charge, and lower for negatively charged atoms. Final state effects refer to electronic relaxation that occurs as the photoelectron is ejected, lowering the energy of the final core-hole state, thus decreasing the measured binding energy. Several types of relaxation processes are possible depending on the nature of the sample. Even in isolated atoms, the orbital energies drop in response to the presence of the core hole, resulting in a net binding energy less than the negative of the core orbital energy. If the emitting atom is part of a bulk metal or large

supported metal particle, the positive atomic charge is neutralized or screened by movement of conduction electrons. This screening results in substantial lowering of the binding energy, relative to that observed for isolated atoms. Atoms or small clusters supported on insulating or semiconducting supports are an intermediate case, where screening is primarily by polarization of neighboring atoms or by intra-cluster electronic relaxation. The binding energies in this case are significantly higher than in the bulk metal, but still well below the value for isolated atoms.

For all our samples, the Au XPS binding energies are higher than for bulk gold (84.3 eV). In principle, the shift to higher binding energy relative to the bulk could result from gold being in a positive oxidation state (i.e., from an initial state effect). A gold formal positive oxidation state is quite unlikely, however, because the gold ionization energy (9.226 eV [33]) is much larger than the TiO<sub>2</sub> band gap (3.05 eV [34]). In all our samples, the gold is almost certainly formally in the zero oxidation state, although partial charging may accompany bonding at different sites, as discussed below. The shifts to higher binding energy relative to bulk gold must, therefore, result primarily from final state effects, i.e., from the limited screening possible for Au atoms or small Au clusters dispersed on the TiO<sub>2</sub> support.

For  $T_{\text{anneal}} \geq 450$  K, we observe the main XPS component to have a binding energy of 84.5 eV, i.e., ~0.2 eV higher than bulk gold. Howard et al. [32] measured Au 4f binding energies for Au/TiO<sub>2</sub>, and found the bulk limit was reached for ~5 ML Au overlayers. For decreasing gold coverage, the binding energy increased, reaching 84.5 eV for their lowest coverage (0.1 ML). An earlier STM study by the same group indicated that the 0.1 ML room temperature sample contained gold clusters with average size around 2 nm [16]. These results, therefore, are consistent with our assignment of the 84.5 eV fit component to Au in clusters. The fact that we observe significant contribution from the 84.5 eV fit component only after annealing above room temperature is further evidence that agglomeration behavior for our samples is different from that observed for evaporated gold.

The high binding energy (85.8 eV) attributed to atomically-dispersed Au for  $T_{\text{anneal}} \leq 200$  K is consistent with the minimal screening possible for isolated atoms on  $\text{TiO}_2$ . In addition, several computational studies have suggested that partial electron transfer may occur from Au to the stoichiometric  $\text{TiO}_2$  surface, and this partial positive charge would certainly increase the XPS binding energy [31,35].

If our assignment of the 85.4 eV binding energy component ( $T_{\text{anneal}} = 300$  K) to Au–vacancy complexes is correct, then this implies that Au bound to vacancies either is more negatively charged, or that there is additional final state relaxation, relative to Au on stoichiometric  $\text{TiO}_2$  sites. The vacancies are electron-rich sites, thus both charging and enhanced relaxation effects may be important. Decreased Au 4f binding energies were also observed by Howard et al. [32], for gold evaporated onto a  $\text{TiO}_2$  surface with high defect density.

The large Au XPS shifts observed for as-deposited Au could also occur if some AuTi or Au oxide compound were forming in our hyperthermal deposition process, but some evidence of compound formation should also appear in the Ti XPS. Fig. 4 shows Ti 2p XPS taken under the same conditions as Fig. 2. For the clean  $\text{TiO}_2$  support, there is a large peak for  $\text{Ti}^{4+}$ , and a weak shoulder corresponding to  $\text{Ti}^{3+}$  (oxygen vacancies). There

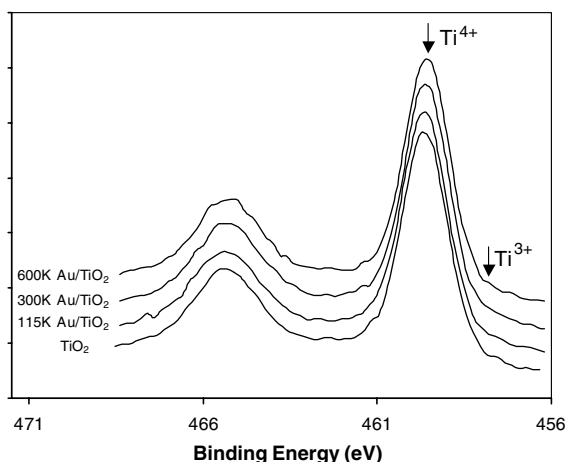


Fig. 4. Ti 2p XPS for  $\text{TiO}_2$  and for Au/ $\text{TiO}_2$  annealed to different temperatures.

are no significant changes resulting from deposition of 0.05 ML-equivalent of  $\text{Au}^+$  at 115 K, or from annealing up to 600 K, indicating that compound formation or other dramatic changes in Ti formal oxidation state are not occurring. Ti XPS is probably not sensitive enough to show the effects of partial electron transfer with Au. The problem is that unlike Au XPS, where all emitting atoms are on the surface, Ti XPS probes the top few nanometers of the sample. Because Ti atoms bonding to the 0.05 ML-equivalent of gold make up only a small fraction of the Ti probed, only large shifts are expected to be observable.

### 3.3. CO adsorption effects on XPS and CO temperature-programmed desorption (TPD)

The effects of CO adsorption on the XPS binding energies were also probed in a separate set of experiments shown in Fig. 5. Pairs of spectra are shown, along with fits. For each pair, 0.05 ML-equivalent of  $\text{Au}^+$  was deposited at 1 eV and 115 K surface temperature, then annealed to the specified temperature for 5 min and re-cooled to 115 K. The lower spectrum of each pair was taken immediately after annealing, without CO exposure. The samples were then exposed to 5 L of CO at 115 K, and re-examined by XPS (upper spectra in each pair). Fitting of the pre-CO-exposure spectra was done as in Fig. 1. Fitting of the post-CO spectra is discussed below.

As-deposited Au at 115 K, where most Au is in the form of isolated atoms, gives a broad XPS feature with peak binding energy of 85.8 eV. After exposure to CO at 115 K, the peak broadens and shifts to higher binding energy, with peak binding energy of 86.7 eV. This large shift indicates that CO adsorption on isolated atoms strongly perturbs the Au electronic environment. The breadth of the XPS feature indicates considerable heterogeneity in the resulting Au chemical environment.

For the sample annealed to 300 K for 5 min, the pre-CO-exposure XPS peaks is dominated by the 85.4 eV fit component assigned to Au–vacancy complexes. Subsequent CO exposure does not shift the peak position, however, the peak intensity decreases slightly and there clearly is a new shoulder at higher binding energy. The shoulder is not

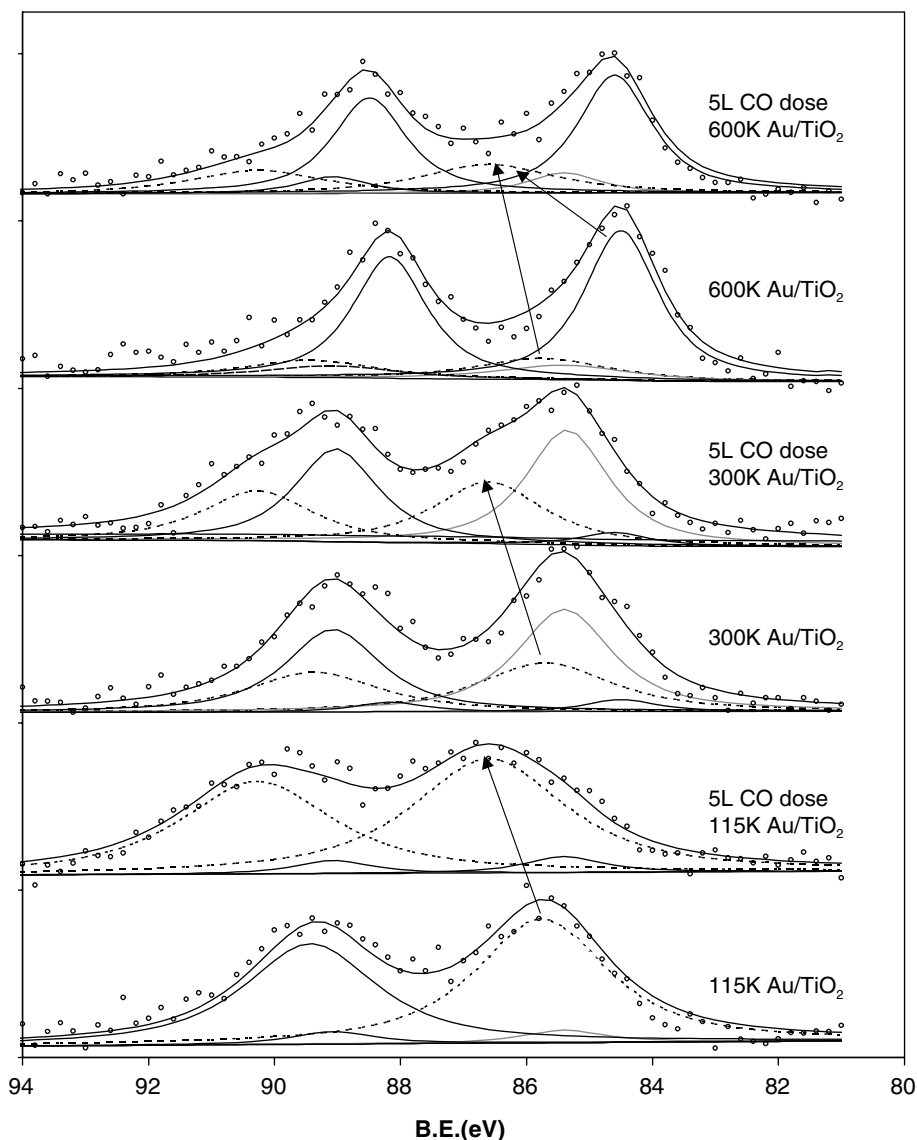


Fig. 5. Au4f XPS for Au/TiO<sub>2</sub> with the different annealing temperature (115 K, 300 K, 600 K), before and after a 5 L CO exposure at 115 K. Fitting is described in the text.

resolved, however, its position is consistent with the 86.7 eV peak observed for the unannealed sample after CO exposure. This pattern suggests that the 300 K sample has at least two types of Au atoms, consistent with the fitting results in Fig. 2. Gold initially present as isolated atoms is strongly affected by CO binding, giving rise to the 86.7 eV shoulder. Gold in vacancy complexes is weakly

perturbed by CO exposure, giving rise to the unshifted peak at 85.4 eV.

Finally, for the sample annealed to 600 K, the pre-CO-exposure spectrum has a sharp peak with binding energy of 84.5 eV, attributed to Au in supported clusters. Upon CO exposure, the 84.5 eV peak is unshifted, but decreases in intensity. This missing intensity appears at higher binding

energies ( $\sim 86.7$  eV), filling in the gap between the fine structure peaks. Absence of a shift in the main peak could indicate that CO does not adsorb on supported Au clusters at 115 K, or simply that the CO-induced change in binding energy is within our relatively poor energy resolution.

The fits to the post-CO spectra are based on the observation that CO adsorption on isolated atoms strongly shifts the XPS to higher binding energy, while the shifts are small for CO adsorbing on Au in clusters or in the 85.4 eV fit component. The fit to the 115 K spectra, therefore, simply allowed the pre-CO component for isolated atoms (85.8 eV) to shift to a best fit binding energy of 86.7 eV, while the small 85.4 eV component was assumed to be unchanged by CO adsorption. Similarly, the 300 K spectrum was fit by allowing the isolated atom (85.8 eV) component to shift to 86.7 eV, leaving the 85.4 eV (vacancy) component and the minor 84.5 eV (cluster) components unshifted. The integrated intensities of the two main components changed by only a few percent.

The 600 K post-CO fit also allowed the isolated atom component to shift to 86.7 eV, however, the fraction of isolated atoms present after 600 K annealing is too small to account for the substantial 86.7 eV intensity following CO exposure. Because it is clear that the intensity of the main 84.5 eV component decreases upon CO exposure, we allowed a fraction of this intensity to shift to the post-CO 86.7 eV component. This shift corresponds to a decrease in the fraction of CO present as clusters, with concomitant increase in CO bound to isolated atoms, suggesting that there is some CO-induced disruption of small Au particles. Such CO-induced particle breakup has been observed in other supported clusters systems, e.g., Ir/titania [36], Ru/alumina [37], Rh/alumina [38] and Rh/silica [39]. We are not aware of analogous experiments for small  $\text{Au}_n/\text{TiO}_2$ , however, the STM work of Kolmakov and Goodman [40] does demonstrate that small ( $\sim 1$  nm) Au particles are disrupted by a CO–O<sub>2</sub> mixture under CO oxidation reaction conditions. In that experiment there were also large (4 nm) Au particles present, and the gold from the disrupted clusters appeared to add to the large particles in an adsorbate-enhanced ripening process.

The Blyholder model [41] is often used to rationalize chemical shifts of metal XPS induced by CO adsorption. In this model, the metal–CO bonding is broken down into two components. A  $\sigma$  bond is formed by electron transfer from the filled  $5\sigma$  orbital of CO to unfilled metal orbitals, and a  $\pi$  bond is formed by back donation of metal d-electrons to the empty  $2\pi^*$  orbital of CO. XPS chemical shifts are sensitive to changes in electron densities, and are, thus, useful in probing the relative contributions from  $\sigma$  bonding and  $\pi$  back-bonding. CO-induced core level shifts have been well studied, for example on Pd single crystals [42] and supported Pd particles [43,44], however, we are not aware of analogous studies for CO on gold particles. The observation that CO adsorption on isolated Au atoms leads to a large XPS shift to higher binding energy, indicates that Au loses electron density in CO–Au bond formation. In the Blyholder model, this net electron transfer out of Au would be rationalized in terms of a  $\pi$  back donation larger than the  $\sigma$  donation. This interpretation is consistent with a study using UPS and infrared spectroscopy by Meier et al. [45] for CO on Au(110)-(1  $\times$  2), which suggested relatively weak CO  $\sigma$  contributions, compared to the metal-to-CO  $\pi$  back donation. On the other hand, a recent DFT calculation by Vittadini and Selloni [46] found that while Au adatoms developed a partial positive charge (+0.33) upon CO adsorption, the electron density transferred to the TiO<sub>2</sub> substrate, rather than to the CO. This calculation is consistent with our observation of a large shift to higher Au 4f binding energy upon CO adsorption on isolated Au atoms.

The absence of observable XPS shifts for CO adsorbing on gold clusters or gold–vacancy complexes, indicates that CO bonding to Au in these environments causes a substantially weaker perturbation than for isolated Au atoms. In the Blyholder model, this effect would be taken as evidence for weaker  $\pi$  back-bonding, compared to CO on Au bound to stoichiometric sites. Weaker CO bonding to Au–vacancy complexes is also predicted by the calculations of Vittadini and Selloni [46], although their calculations also predict that the Au in a CO–Au–vacancy complex has a significant positive charge. Unless there is also a

compensating decrease in final state relaxation, this positive charge would result in a shift to higher binding energy, which is not observed.

The conclusion that CO adsorbs more weakly to Au–vacancy complexes is supported by CO TPD experiments. Samples were prepared as above by Au<sup>+</sup> deposition at 115 K, annealed to various temperatures for 5 min, then re-cooled and exposed to 5 L of CO. TPD was measured over the temperature range from ~160 K to 350 K. As shown in Fig. 6, CO adsorbed on as-deposited Au/TiO<sub>2</sub> at 115 K desorbs in a broad peak centered at ~280 K. For the sample annealed to 300 K, the peak shifts to lower temperatures, and the amount of CO desorbing is reduced to ~60% of the amount desorbing from the unannealed sample. Desorption in the temperature range between ~230 and 350 K presumably originates from CO adsorbed on the fraction of Au still present as isolated atoms after the 300 K anneal, and the decreased peak temperature represents CO binding more weakly to Au–vacancy complexes. After annealing to 600 K, the amount of CO desorbing is reduced to only ~40% of the amount desorbing from the unannealed sample, and the desorption maximum is near 200 K. The lack of desorption in the 230–350 K range is consistent with the near absence of isolated atoms (85.8 eV XPS component in Fig. 3) after 600 K annealing, and the peak around 200 K presumably results from CO bound to Au clusters.

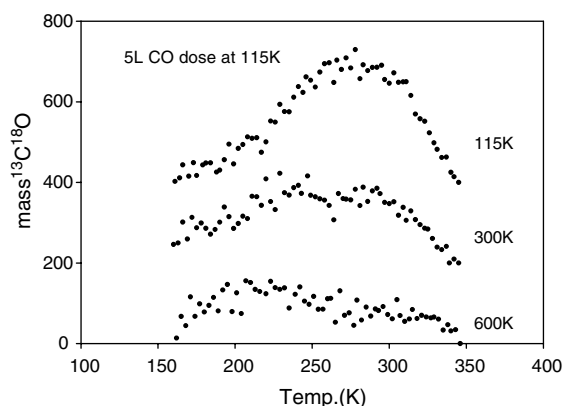


Fig. 6. <sup>13</sup>C<sup>18</sup>O TPD spectra for samples annealed to various temperatures prior to 5 L exposure to <sup>13</sup>C<sup>18</sup>O at 115 K.

The 280 K CO desorption observed for as-deposited Au is considerably higher than what is seen in gold single crystal studies. For example, a CO adsorption study on Au(110)-(1 × 2) by Gottfried et al. showed desorption peaks at 37, 67, and 145 K, and even on a surface roughened by ion bombardment the highest temperature desorption feature was at 185 K [21]. On the other hand, a sample prepared by evaporation of 0.2 Å of Au on FeO(111) and Fe<sub>3</sub>O<sub>4</sub> (111) by Lemire et al., showed CO desorption peaks at 280 K and 300 K [18]. In that experiment, STM at room temperature showed formation of small Au clusters, however, the TPD experiments were done on samples with gold deposited at low temperature, so that the Au was probably atomically dispersed during CO exposure. They also found that annealing the samples at 500 K prior to CO exposure, lead to formation of ~2 nm size Au clusters, and loss of the high temperature desorption peak. Similarly, in an FTIR study of CO adsorption on Au/TiO<sub>2</sub>, Boccuzzi et al. [47] inferred strong CO–Au bonding in small Au clusters, based on the observed red-shifted 2055 cm<sup>-1</sup> CO vibrational peak.

Our interpretation of these results requires that CO bind more tightly to Au atoms in stoichiometric TiO<sub>2</sub> sites than to Au–vacancy complexes or Au clusters. Previous work suggests that at least two factors are at work. The experiments by Gottfried et al. on roughened Au(110) suggest that CO binds more strongly to low coordination gold atoms [21], and dispersed atoms are obviously the low-coordination limit. On the other hand, CO bonding to Au complexed to a vacancy has been calculated to be weak [7,46]. This result was rationalized in terms of the vacancies transferring negative charge to the Au atoms (observed as decreased Au4f binding energy, Fig. 2), weakening the σ component of the CO–Au bond.

### 3.4. Comparison with damaged TiO<sub>2</sub>

Given our tentative conclusion that the 85.4 eV Au4f binding energy is associated with Au bound to vacancies, an obvious test is to examine binding energies for Au on a surface with higher vacancy concentration. Additional oxygen vacancies (along with other, uncharacterized defects) were created

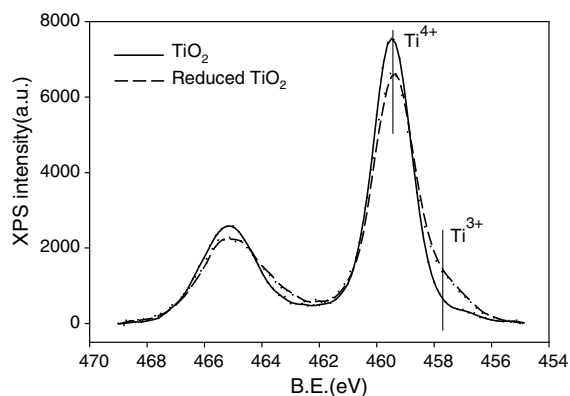


Fig. 7. Ti 2p XPS of UHV-annealed TiO<sub>2</sub> (“TiO<sub>2</sub>”) and TiO<sub>2</sub> bombarded by He<sup>+</sup> to create additional oxygen vacancies (“reduced TiO<sub>2</sub>”).

by 1 keV He<sup>+</sup> bombardment (600 nA ion current, 10 min exposure). Fig. 7 shows Ti 2p XPS spectra taken before and after He<sup>+</sup> bombardment. Note the reduction in Ti<sup>4+</sup> intensity, and accompanying increase in Ti<sup>3+</sup> intensity (to ~12% of the total Ti signal), indicating creation of additional oxygen vacancies in the near-surface region. ISS scans run just before and after the He<sup>+</sup> bombardment show a decrease in oxygen ISS intensity of 16%—significantly larger than the 12% Ti<sup>3+</sup> XPS intensity. The difference reflects the different sample depths probed by XPS (top few nanometers) and ISS (top layer only), and suggests that the oxygen vacancy concentration is somewhat higher on the surface than in the near-surface region.

Fig. 8 shows two pairs of Au 4f spectra for Au<sup>+</sup> deposited at 115 K. The bottom set is for UHV-annealed (low vacancy density) TiO<sub>2</sub>, and top set is for He<sup>+</sup>-bombarded TiO<sub>2</sub> (denoted TiO<sub>2-x</sub>). In each pair, the bottom spectrum was taken just after Au deposition, and the top spectrum was taken after subsequent exposure to 5 L of CO, also at 115 K. On the He<sup>+</sup>-bombarded surface, the pre-CO-exposure Au 4f binding energy is shifted slightly to lower binding energy, compared to the UHV-annealed surface. The increased breadth presumably reflects increased heterogeneity in Au bonding environments. In particular, the higher density of oxygen vacancies means that the chances of Au landing and binding at a vacancy

site is significantly increased. The vacancies are electron rich sites, thus vacancy-bound Au will tend have increased electron density, with concomitant shift to of the average XPS binding energy. Similar binding energy shifts were also observed by Howard et al. [32], for Au evaporated onto a high defect density TiO<sub>2</sub> surface.

The pre-CO spectrum for Au/damaged TiO<sub>2</sub> can be fit with the same three components as the spectra for undamaged TiO<sub>2</sub>, with only changes in the relative component intensities. As for the undamaged TiO<sub>2</sub>, there is a component at 85.8 eV, assigned to isolated Au on TiO<sub>2</sub> sites, however, this component is no longer dominant. Instead, there is roughly equal contributions from the 85.8 and 85.4 eV components. This change is exactly what would be expected if the 85.4 eV component represents Au–vacancy complexes, because the vacancy concentration is much higher on the damaged surface.

Fig. 8 also shows that the two samples respond differently to CO adsorption. As noted above, for Isolated Au on stoichiometric sites (i.e., the 85.8 eV pre-CO component), there is a shift to 86.7 eV binding energy, reflecting the strong CO–Au bond. The 85.4 eV component, assigned to Au bound at oxygen vacancies, was shown not to shift significantly upon CO exposure (Fig. 5, 300 K results). The effect of CO exposure on the Au/damaged TiO<sub>2</sub> sample is completely consistent. The ~50% of Au present as atoms on stoichiometric sites binds strongly to CO, leading to a component at 86.7 eV, while the other half of the Au atoms, bound at vacancies, continues to generate an unshifted 85.4 eV component.

#### 4. Conclusions

In summary, the evidence bearing on the nature of the samples resulting from Au<sup>+</sup> deposited on TiO<sub>2</sub> at room temperature, or annealed to room temperature consists of the following:

(1) Room temperature CO oxidation on model catalysts prepared by Au<sub>n</sub><sup>+</sup> deposition under conditions identical to those used here, is strongly dependent on cluster size. In particular, catalysts

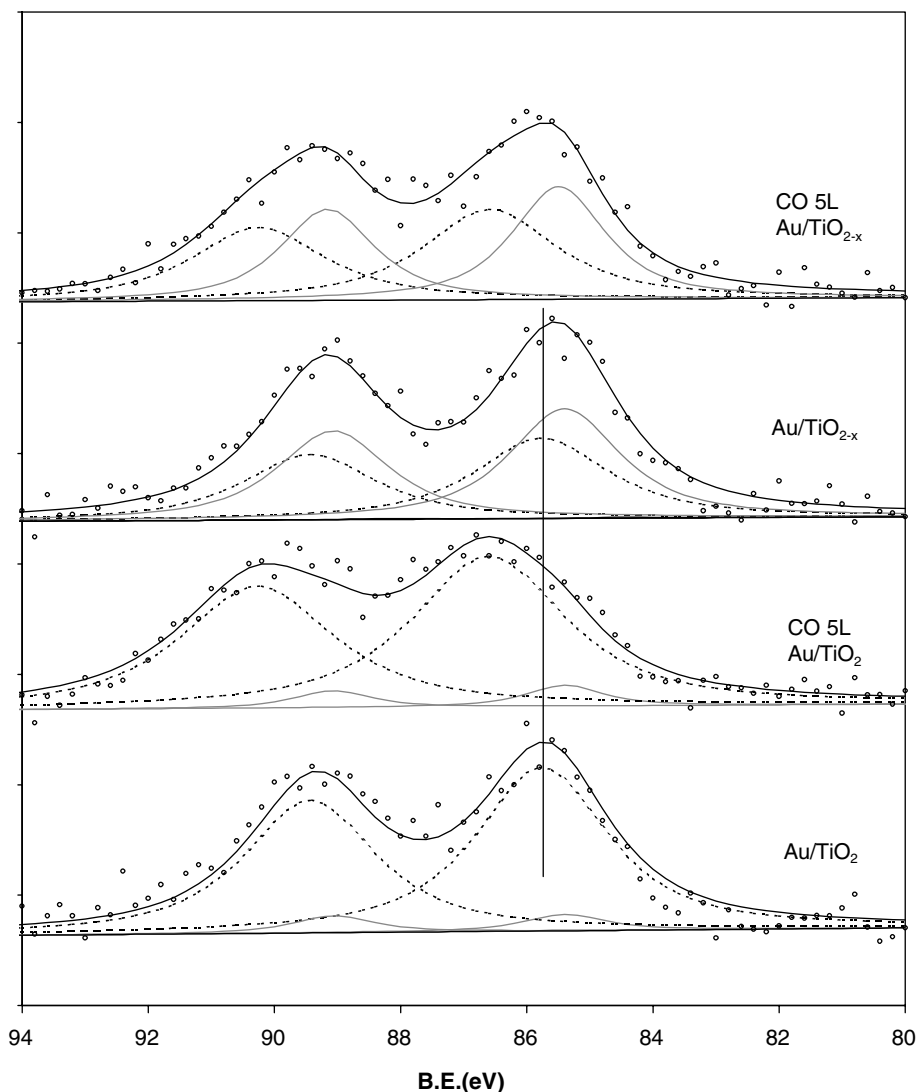


Fig. 8. Comparison of Au4f XPS for Au deposited on UHV-annealed  $\text{TiO}_2$  ( $\text{Au/TiO}_2$ ) and on  $\text{He}^+$ -bombarded  $\text{TiO}_2$  with additional oxygen vacancies ( $\text{Au/TiO}_{2-x}$ ), before and after a 5 L CO exposure at 115 K. Fitting is described in the text.

prepared by deposition of  $\text{Au}_3^+$  or larger clusters are active. The dramatic size effects seem to preclude significant agglomeration at temperatures up to 300 K.

(2) Catalysts prepared by  $\text{Au}_1^+$  or  $\text{Au}_2^+$  deposition are substantially less active than  $\text{TiO}_2$  itself. The  $\text{TiO}_2$  activity is attributed to reaction at vacancies, thus  $\text{Au}_1$  and  $\text{Au}_2$  appear to poison (i.e. bind at) vacancy sites.

(3) ISS Au/substrate ratios are temperature independent up to 300 K, indicating that the dispersion of gold on the surface is not changed significantly. Significant decreases occur in the Au/substrate ratios for  $T_{\text{anneal}} \geq 450$  K, consistent with agglomeration becoming important only above room temperature.

(4) Annealing of model catalysts prepared by  $\text{Au}^+$  deposition to temperatures above 400 K does

result in substantial activity, consistent with the ISS finding that agglomeration becomes important in temperature range.

(5) XPS shows evidence of three stages in the thermal modification of the as-deposited low temperature Au/TiO<sub>2</sub> samples. A single Au 4f peak at 85.8 eV, assigned to Au on stoichiometric TiO<sub>2</sub> sites, is observed for temperatures up to 200 K. At 300 K the main peak has shifted to 85.4 eV, and is assigned to Au–vacancy complexes. At 450 K and higher temperatures, the Au 4f spectrum is dominated by a peak at 84.5 eV, assigned to Au in clusters.

(6) For Au deposited on TiO<sub>2</sub> with a high density of oxygen vacancies, the Au XPS spectrum similar to that measured on UHV-annealed TiO<sub>2</sub> after annealing to 300 K. In particular, the 85.4 eV component dominates in both cases.

(7) The effects of CO adsorption on Au 4f binding energy also indicate a significant change in Au properties occurring by 300 K. For as-deposited gold, there is a large shift and broadening to high binding energy induced by upon CO adsorption, consistent with strong CO bonding to isolated Au on stoichiometric sites. For samples annealed to 300 K, or for Au on the high-vacancy-concentration surface, the binding energy shifts are small, consistent with weaker CO bonding Au–vacancy complexes. CO TPD experiments are consistent with this interpretation.

While we do not claim to know the detailed nature of the Au binding sites, we feel that the evidence clearly shows that the samples prepared by Au<sup>+</sup> deposition at room temperature consist mainly of Au bound to vacancy sites, with lower concentrations of Au in other binding sites or in small clusters. This result is apparently in major disagreement with the STM experiments on gold evaporated onto rutile TiO<sub>2</sub>(110), where clusters of tens of atoms are observed at room temperature [4,16]. In reality, the experiments do not differ so dramatically. Our XPS results (Fig. 3) suggest that there is a small amount of agglomeration to small clusters (the 84.5 eV component) even at 300 K. Both CO oxidation and ISS indicate that even mild annealing is sufficient to induce significant agglomeration, thus it appears that the room temperature is near the limit where strong size depen-

dence could be observed for Au<sub>n</sub><sup>+</sup> deposited on TiO<sub>2</sub>.

The question remains, why agglomeration appears to be more facile in the evaporated gold samples. The difference could result from different densities of vacancies on the TiO<sub>2</sub>, although the preparation conditions are nominally almost identical, as are the reported vacancy densities. More likely, the effect results from damage to the TiO<sub>2</sub> from deposition of Au<sup>+</sup> at 1 eV/atom. This impact energy does not appear to be high enough to sputter the surface, as shown by unchanging O and Ti XPS spectra, but it may cause some local disorder that reduces mobility on the surface. This would account for why our sample only begin to show evidence for agglomeration above room temperature.

## Acknowledgment

We gratefully acknowledge support by grant DE-FG03-99ER15003 from the Chemical Sciences, Geosciences and Biosciences Division, Office of Basic Energy Sciences, Office of Science, US Department of Energy.

## References

- [1] M. Haruta, Catal. Today 36 (1997) 153.
- [2] M. Valden, X. Lai, D.W. Goodman, Science 281 (1998) 1647.
- [3] V.A. Bondzie, S.C. Parker, C.T. Campbell, Catal. Lett. 63 (1999) 143.
- [4] E. Wahlstrom, N. Lopez, R. Schaub, P. Thostrup, A. Ronnau, C. Africh, E. Laegsgaard, J.K. Nørskov, F. Besenbacher, Phys. Rev. Lett. 90 (2003) 026101/1.
- [5] S. Lee, C. Fan, T. Wu, S.L. Anderson, J. Am. Chem. Soc. 126 (2004) 5682.
- [6] N. Lopez, J.K. Nørskov, Surf. Sci. 515 (2002) 175.
- [7] L.M. Molina, M.D. Rasmussen, B. Hammer, J. Chem. Phys. 120 (2004) 7673.
- [8] Z. Yang, R. Wu, D.W. Goodman, Phys. Rev. B 61 (2000) 14066.
- [9] Z.-P. Liu, X.-Q. Gong, J. Kohanoff, C. Sanchez, P. Hu, Phys. Rev. Lett. 91 (2003) 266102.
- [10] G.R. Bamwenda, S. Tsubota, T. Nakamura, M. Haruta, Catal. Lett. 44 (1997) 83.
- [11] J.-D. Grunwaldt, A. Baiker, J. Phys. Chem. B 103 (1999) 1002.

- [12] B. Schumacher, V. Plzak, M. Kinne, R.J. Behm, *Catal. Lett.* 89 (2003) 109.
- [13] J.M.C. Soares, P. Morrall, A. Crossley, P. Harris, M. Bowker, *J. Catal.* 219 (2003) 17.
- [14] Y.-S. Su, M.-Y. Lee, S.D. Lin, *Catal. Lett.* 57 (1999) 49.
- [15] A. Sanchez, S. Abbet, U. Heiz, W.-D. Schneider, H. Häkkinen, R.N. Barnett, U. Landman, *J. Phys. Chem. A* 103 (1999) 9573.
- [16] C.E.J. Mitchell, A. Howard, M. Carney, R.G. Egdell, *Surf. Sci.* 490 (2001) 196.
- [17] S. Arrii, F. Morfin, A.J. Renouprez, J.L. Rousset, *J. Am. Chem. Soc.* 126 (2004) 1199.
- [18] C. Lemire, R. Meyer, S.K. Shaikhutdinov, H.-J. Freund, *Surf. Sci.* 552 (2004) 27.
- [19] S.K. Shaikhutdinov, R. Meyer, M. Naschitzki, M. Bäumer, H.-J. Freund, *Catal. Lett.* 86 (2003) 211.
- [20] N. Lopez, J.K. Nørskov, *J. Am. Chem. Soc.* 124 (2002) 11262.
- [21] J.M. Gottfried, K.J. Schmidt, S.L.M. Schroeder, K. Christmann, *Surf. Sci.* 536 (2003) 206.
- [22] K.J. Boyd, A. Lapicki, M. Aizawa, S.L. Anderson, *Rev. Sci. Instrum.* 69 (1998) 4106.
- [23] M. Aizawa, S. Lee, S.L. Anderson, *J. Chem. Phys.* 117 (2002) 5001.
- [24] M. Aizawa, S. Lee, S.L. Anderson, *Surf. Sci.* 542 (2003) 253.
- [25] W.S. Epling, C.H.F. Peden, M.A. Henderson, U. Diebold, *Surf. Sci.* 412/413 (1998) 333.
- [26] R.W.M. Kwok, XPSPEAK, Shatin, 1998.
- [27] J.W. Rabalais, *Principles and Applications of Ion Scattering Spectrometry: Surface Chemical and Structural Analysis*, Wiley, New York, 2003.
- [28] S. Lee, C. Fan, T. Wu, S.L. Anderson, in preparation.
- [29] X. Lai, T.P. St. Clair, M. Valden, D.W. Goodman, *Prog. Surf. Sci.* 59 (1998) 25.
- [30] J.R. Kitchin, M.A. Barteau, J.G. Chen, *Surf. Sci.* 526 (2003) 323.
- [31] A. Vijay, G. Mills, H. Metiu, *J. Chem. Phys.* 118 (2003) 6536.
- [32] A. Howard, D.N.S. Clark, C.E.J. Mitchell, R.G. Egdell, V.R. Dhanak, *Surf. Sci.* 518 (2002) 210.
- [33] H.-P. Looock, L.M. Beaty, B. Simard, *Phys. Rev. A* 59 (1999) 873.
- [34] D.C. Cronmeyer, *Phys. Rev.* 87 (1952) 876.
- [35] L. Giordano, G. Pacchioni, T. Bredow, J.F. Sanz, *Surf. Sci.* 471 (2001) 21.
- [36] A. Berko, F. Solymosi, *Surf. Sci.* 411 (1998) L900.
- [37] T. Mizushima, K. Tohji, Y. Udagawa, A. Ueno, *J. Phys. Chem.* 94 (1990) 4980.
- [38] H.F.J. Van't Blik, J.B.A.D. Van Zon, T. Huizinga, J.C. Vis, D.C. Koningsberger, R. Prins, *J. Phys. Chem.* 87 (1983) 2264.
- [39] P. Basu, D. Panayotov, J.T. Yates Jr., *J. Phys. Chem.* 91 (1987) 3133.
- [40] A. Kolmakov, D.W. Goodman, *Surf. Sci.* 490 (2000) L597.
- [41] G. Blyholder, *J. Phys. Chem.* 68 (1964) 2772.
- [42] J.N. Andersen, M. Qvarford, R. Nyholm, S.L. Sorensen, C. Wigren, *Phys. Rev. Lett.* 67 (1991) 2822.
- [43] A. Sandell, J. Libuda, P.A. Brühwiler, S. Andersson, M. Bäumer, A.J. Maxwell, N. Martensson, H.J. Freund, *Phys. Rev. B* 55 (1997) 7233.
- [44] A. Sandell, J. Libuda, P.A. Bruehwiler, S. Andersson, A.J. Maxwell, M. Bäumer, N. Maertensson, H.J. Freund, *J. Vac. Sci. Technol. A* 14 (1996) 1546.
- [45] D.C. Meier, V. Bukhtiyarov, D.W. Goodman, *J. Phys. Chem. B* 107 (2003) 12668.
- [46] A. Vittadini, A. Selloni, *J. Chem. Phys.* 117 (2002) 353.
- [47] F. Boccuzzi, A. Chiorino, M. Manzoli, *Surf. Sci.* 454–456 (2000) 942.